Check for updates

LIMNOLOGY AND OCEANOGRAPHY
Letters

ASLO
Open Access

Limnology and Oceanography Letters 3, 2018, 393–400
© 2018 The Authors. Limnology and Oceanography published by Wiley Periodicals, Inc. on behalf of Association for the Sciences of Limnology and Oceanography.
doi: 10.1002/lol2.10090

LETTER

Ocean acidification can interact with ontogeny to determine the trace element composition of bivalve shell

C. R. Norrie [1]* *B. J. Dunphy,* [1,2] *N. L. C. Ragg,* [3] *C. J. Lundquist* [1,4]

[1]Institute of Marine Science, University of Auckland, Auckland, New Zealand; [2]School of Biological Sciences, University of Auckland, Auckland, New Zealand; [3]Cawthron Institute, Nelson, New Zealand; [4]National Institute of Water and Atmospheric Research (NIWA), Hamilton, New Zealand

Scientific Significance Statement

The trace element composition of the calcium carbonate ($CaCO_3$) structures of organisms, such as bivalve shells or fish otoliths, can provide information on the physical and chemical properties of the water in which it is formed. Ocean acidification, from increases in anthropogenic CO_2, changes the ocean's carbonate chemistry; however, it is unclear how it might influence trace elemental incorporation into carbonate structures. This study provides evidence that 13 out of 17 elements tested in Greenshell™ mussels are affected by pCO_2, but that it differed by shell age. Our results suggest that elements in young shells are stable under different pCO_2 levels and can be used to determine dispersal histories, but older shell could be used to reconstruct carbonate chemistry.

Abstract

We sought to determine how pCO_2 will affect the incorporation of trace elements into bivalve shell. This was to validate that under high pCO_2 conditions reconstruction of animal movements is still viable; and to investigate potential trace element proxies for ocean carbonate chemistry. Here, we examined shell of the bivalve *Perna canaliculus* formed under current CO_2 ($pCO2$ = 400 µatm) conditions and those predicted to exist in 2100 ($pCO2$ = 1050 µatm). Seventeen trace element:calcium ratios were examined at two locations within shells. Elements that are typically most useful in determining connectivity patterns (e.g., Sr, Mn, Ba, Mg, B) were not affected by pCO_2 in shell produced early in individual's lives. This suggests that the effects of ocean acidification on dispersal signatures may be dampened. However, cobalt, nickel, and titanium levels were influenced by pCO_2 consistently across shells suggesting their role as potential indicators of CO_2 level.

The trace elemental composition of biogenic calcium carbonate ($CaCO_3$) structures such as shells or otoliths reflect the physicochemical properties of the water in which they are formed (Beer et al. 2011; Poulain et al. 2015). Therefore, the trace elemental composition of $CaCO_3$ structures can provide valuable information on the water mass in which they were produced. Currently, there are two primary areas in which this information is applied: population connectivity and paleoclimate reconstructions. Variations in multiple trace elements in bivalve shells, gastropod statoliths, and fish otoliths have been used to infer dispersal histories, population connectivity and stock structure, a technique known as trace elemental fingerprinting (,Gomes et al. 2016; Kroll et al. 2016). Among climate researchers, there is also interest in the use of the elemental composition of $CaCO_3$ structures as proxies to reconstruct environmental conditions such as temperature, salinity or pH at their time and location of formation (Poulain et al. 2015, Immenhauser et al. 2016).

*Correspondence: craig.norrie@auckland.ac.nz

Author contribution statement: CN with input from all authors wrote the manuscript. CN performed trace elemental work and analyzed results. NR conducted the animal culturing and sampling. All authors discussed results and contributed to drafts of the manuscript.

Data availability statement: Data are available in the Figshare repository at https://doi.org/10.17608/k6.auckland.6118745.v1.

Additional Supporting Information may be found in the online version of this article.

This is an open access article under the terms of the Creative Commons Attribution License, which permits use, distribution and reproduction in any medium, provided the original work is properly cited.

Ocean acidification (OA) is the decrease in ocean pH, due to the uptake of anthropogenic CO_2 from the atmosphere. Once dissolved into seawater, CO_2 increases the concentration of bicarbonate ions ($[HCO_3^-]$) and lowers the pH and concentration of the carbonate ion ($[CO_3^{2-}]$) (Gattuso and Hansson 2011). In addition to this change in the carbonate equilibrium reaction, the availability of ions will also be affected (Millero et al. 2009). As the incorporation of trace elements into biogenic $CaCO_3$ is affected by both the availability of ions and a number of other environmental and physiological processes (Beer et al. 2011), the composition of these carbonate structures is likely to be affected by changes in oceanic pH (Hoffmann et al. 2012; Frieder et al. 2014, Levin et al. 2015).

Understanding how OA affects the trace elemental composition of carbonate structures will provide valuable information for both trace elemental fingerprinting and climate reconstructions. If the trace elemental composition of shell material is to be used to reconstruct the pH history of the oceans, any proxies that are used should have a defined and stable relationship with pH (Yu et al. 2007; Henehan et al. 2013). For trace elemental fingerprinting, understanding how OA will affect trace elemental incorporation into carbonate structures will allow us to ensure this technique remains viable under future conditions. Currently, differences in shell chemistry caused by physicochemical properties such as temperature, salinity, and the availability of elements in the surrounding environment are used to assign shells to their origin (Becker et al. 2007; Kroll et al. 2016). If the effects of pH on the composition of shell material are unknown the possibility that any differences observed are erroneously attributed to other environmental variables exists. In addition, many estuarine and coastal environments experience seasonal or diel changes in pH (Law et al. 2017), which could complicate reconstructions of both climactic conditions and larval dispersal without a solid understanding of how this variation influences shell chemistry.

The possibility also exists for these largely separate applications of $CaCO_3$ trace elemental composition to be combined. The suite of trace elements used in trace elemental fingerprinting studies does not frequently overlap with the elements used in climate reconstructions (Dunphy et al. 2011; Hahn et al. 2012; Poulain et al. 2015; Norrie et al. 2016). If changes in pH influence elements, which are not generally used in trace elemental fingerprinting, it may be possible to use trace elemental fingerprinting techniques to determine the location at which a $CaCO_3$ structure formed and simultaneously infer the environmental conditions at this location using a complementary suite of elements. This could potentially reduce the need to deploy expensive monitoring equipment at a number of locations and examining the ecological consequences of sequential exposure to varying pH conditions at different life history stages (Frieder et al. 2014).

To date the majority of research has focused on the impact of OA on the incorporation of trace elements into foraminiferal tests (Yu et al. 2007, Henehan et al. 2013). Bivalves, however, are more frequently used in trace elemental fingerprinting studies (Dunphy et al. 2011; Gomes et al. 2016). The aim of this study was, therefore, to answer the question "how will predicted future ocean *Perna canaliculus* formed under current CO_2 (pCO_2) affect the incorporation of trace elements into the shell of Greenshell™ mussels *Perna canaliculus*?." We explore implications of pCO_2 on both elements that have been used for elucidating dispersal histories and those elements used to reconstruct geological history.

Methods

Animal spawning and husbandry

To minimize genetic influences, a single full-sibling family of Greenshell™ mussels was examined. Individual male and female mussels were randomly selected from unrelated F2 families raised on long-line aquaculture facilities in the Marlborough Sounds (South Island, New Zealand) as part of the Cawthron *Perna canaliculus* selective breeding program. Thermal shock was used to induce spawning; eggs were diluted to 1000 mL^{-1} in either 400 µatm CO_2 (ambient) or 1050 µatm CO_2 (elevated) seawater and fertilized with sperm at 200 egg^{-1} (Ragg et al. 2010). Prior to transfer to 160 L conical incubation tanks containing 5 µm-filtered seawater and 12 µM EDTA at 16 °C, maintained at 400 µatm CO_2 (ambient) or 1050 µatm CO_2 (elevated) using gentle aeration (air or CO_2 enriched via a gas mixer/analyser (WMA-5; PP Systems, Annesbury, MA). Carbonate conditions in each of the tanks was monitored weekly throughout the course of the experiment (Supporting Information). After 48 h incubation, the embryos had formed the prodissoconch I shell, entering the feeding veliger stage. Larvae were transferred to the continuous-flow culture system described by Ragg et al. (2010). Triplicate 2.5 L control tanks with 200 larvae mL^{-1} received filtered seawater enriched with dietary microalgae (*Tisochrysis lutea* + *Chaetoceros calcitrans*, 40 cells μL^{-1}). After 3 weeks, pediveligers were offered coir string as a settlement substrate and allowed to metamorphose. Juveniles were harvested after 3 months, rinsed in deionized water, snap frozen, and stored (–20 °C) prior to analysis.

Laboratory methods

Methods used were adapted from Norrie et al. (2016). Mussels were defrosted, the shells were split open, and the flesh was removed using stainless steel forceps. Twenty seven individuals raised at 400 µatm CO_2 and 32 raised at 1050 µatm CO_2 were examined.. We selected one valve from each individual at random and fixed it to a glass microscope slide using double sided adhesive tape. To determine the elemental composition of shell material, we performed laser ablation inductively coupled plasma mass spectroscopy (LA-ICP-MS) using a New Wave deep ultra violet (193 nm) laser ablation system (Elemental Scientific Industries, Omaha, Nebraska, USA)

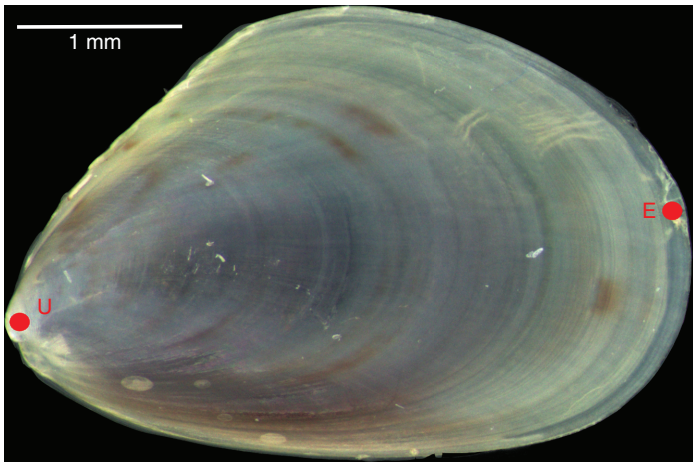

Fig. 1. An example of the juvenile *P. canaliculus* examined in this study. Note: Red dots indicate the locations at which LA-ICP-MS analyses were performed. U indicates the location of analyses performed at the umbo, E indicates analyses performed at the shell edge.

coupled to an Agilent 7700 ICP-MS (Agilent Technologies, Santa Clara, California, USA). Seventeen trace element:calcium ratios were monitored (Li:Ca; B:Ca; Mg:Ca; Al:Ca; Ti:Ca; V:Ca; Mn:Ca; Co:Ca; Ni:Ca; Cu:Ca; Zn:Ca; Sr:Ca; Y:Ca; Ba:Ca; La:Ca; Pb:Ca; U:Ca). We analyzed two locations within the shells; one was located approximately 200 μm from the most recently formed shell edge, and the other was located on the shell umbo (Fig. 1). These locations were selected to represent shell formed early in an individuals life (although our intent was not to sample larval shell formed prior to transfer to the continuous culture system) and as close to the end of the experiment as possible. Background elemental counts were monitored for 30 s prior to each analysis. The laser operated with a spot size of 50 μm, a repetition rate of 5 Hz, and a dwell time of 40 s. We analyzed NIST610 and NIST612 standards every 20 spots for standardization and calibration purposes. Laser power was 45% and the fluence was between 7 and 7.5 Jcm^{-2}. All LA-ICP-MS analyses were performed at The University of Auckland Plasma Mass Spectrometry Centre. Gas flows and voltages were optimized to maximize sensitivity and signal stability while maintaining an oxide reduction ratio of less than 2%; this was monitored using the thorium:thorium oxide ratios. Full laser operating parameters including detection limits and internal precisions are included in the Supporting Information (Tables S1 and S2).

To remove contaminants, we used a pre-ablation technique in which the first 5 s of the laser dwell time were not included in the data reduction process (Marr et al. 2011; Norrie et al. 2016). We used only the next 10 s of data to determine the elemental composition of the shell material to reduce the chances of laser burn through to lower layers within shell material (Strasser et al. 2008). We background corrected data by subtracting background average counts from the ablation average counts. We then converted background corrected counts to trace element:calcium (*TE*:Ca) ratios and standardized them using the most recently published NIST610 values (Jochum et al. 2005). Internal precision was calculated from the NIST612 standard. Finally, *TE*:Ca ratios were converted to μmol:mol ratios, which were used for all statistical analyses.

Statistical analyses

To determine whether differences existed in the incorporation of trace elements into *P. canaliculus* shell under the two pCO_2 conditions we performed univariate statistical analyses on each of the elemental ratios analyzed. All statistical analyses were performed in R version 3.3.3 (R core team). The data did not fit the assumptions of normality; thus, we performed a log transformation on all elemental ratios which improved normality. We used a general linear model (GLM) to examine the effects of the location analyzed within the shell (location), the pCO_2 conditions to which they were exposed (treatment) and any interaction effects. Due to the nested design of this experiment tank was included as a random effect in the GLM. Post hoc t tests were performed, with a FDR *p* value adjustment being performed due to multiple comparisons.

Results

The results of the GLMs indicated that, for 10 of the 17 elemental ratios examined (B:Ca; Mg:Ca; V:Ca; Mn:Ca; Cu:Ca; Sr:Ca; Y:Ca; Ba:Ca; Pb:Ca; U:Ca), there was a significant interaction effect between the location analyzed within shells and the CO_2 treatment to which they were exposed (Table 1). The GLM showed a significant main effect of location within the shell for four *TE*:Ca ratios (Zn:Ca; Li:Ca; Al:Ca; Co:Ca) and a significant main effect of pCO_2 for another three *TE*:Ca ratios (Co:Ca; Ni:Ca; Ti:Ca) (Table 1).The magnitude of differences observed in TE:Ca ratios was highly specific to the element analyzed, the location within shell, and the treatment to which they were exposed. No significant differences were found to exist for Y:Ca ratios after the application of FDR comparisons for multiple corrections.

The results of the post hoc pairwise comparisons showed that Ba:Ca, Cu:Ca, Mn:Ca, and V:Ca ratios differed significantly at the two locations analyzed in shell grown under both ambient and elevated CO_2 conditions (Figs. 2A–D, 3A; Table 1). Ba:Ca, Cu:Ca, and Mn:Ca ratios were significantly higher at the shell edge than at the umbo of animals grown under both elevated and ambient pCO_2. The effect of CO_2 level on the concentration of Ba:Ca, Cu:Ca, and Mn:Ca was dependent on the location within the shell, with higher ratios at the shell edge under ambient pCO_2 and higher ratios at the umbo under elevated pCO_2. V:Ca ratios followed the opposite trend with significantly higher V:Ca ratios at the umbo than

Table 1. Mean (μmol:mol ±SEM) of the *TE*:Ca ratios within shell raised under ambient and predicted future pH conditions. *p* values from the GLM are shown.

Location within shell	*p*CO2 (μatm)	TE:Ca Ratio (μmol/mol)																	
		Li:Ca [1](p = <0.01)	B:Ca [2](p = 0.1)	Mg:Ca [2](p = <0.1)	Al:Ca [1](p = <0.1)	Ti:Ca [3](p = 0.4)	V:Ca [2](p = 0.5)	Mn:Ca [2](p = 0.1)	Co:Ca [3](p = 0.02) [1](p = 0.5)	Ni:Ca [3](p = 0.5)	Cu:Ca [2](p = <0.1)	Zn:Ca [3](p = <0.01)	Sr:Ca [2](p = <0.01)	Y:Ca [2](p = <0.01)	Ba:Ca [2](p = <0.01)	La:Ca	Pb:Ca [2](p = <0.01)	U:Ca [2](p = <0.01)
Edge	400 (Ambient)	2.217	226.661	1546.765	3.424	39.147	0.285	27.563	1.807	2.835	45.794	3.62	4045.062	0.353	8.45	0.013	0.248	0.102
		(±0.081)	(±22.875)	(±129.315)	(±0.999)	(±0.774)	(±0.054)	(±3.346)	(±0.162)	(±0.231)	(±8.021)	(±0.931)	(±118.124)	(±0.033)	(±0.426)	(±0.002)	(±0.071)	(±0.019)
	1050 (Elevated)	2.06	147.063	1164.102	8.297	47.371	0.125	16.218	0.969	1.552	22.066	5.32	3730.231	0.145	6.019	0.025	0.282	0.033
		(±0.1)	(±11.534)	(±146.064)	(±4.114)	(±4.433)	(±0.019)	(±1.44)	(±0.246)	(±0.247)	(±6.037)	(±1.387)	(±129.733)	(±0.01)	(±0.333)	(±0.004)	(±0.058)	(±0.006)
Umbo	400 (Ambient)	1.296	132.057	800.247	11.528	40.647	1.446	7.514	1.78	3.466	4.011	14.652	3548.315	0.304	2.444	0.017	0.279	0.232
		(±0.264)	(±7.904)	(±133.255)	(±2.176)	(±1.155)	(±0.263)	(±0.818)	(±0.188)	(±0.43)	(±0.874)	(±2.551)	(±66.243)	(±0.035)	(±0.167)	(±0.004)	(±0.057)	(±0.028)
	1050 (Elevated)	0.999	134.175	1313.852	17.329	60.903	0.987	9.968	0.778	2.15	4.66	31.403	3977.442	0.187	4	0.092	1.182	0.425
		(±0.106)	(±14.864)	(±243.55)	(±7.214)	(±13.073)	(±0.185)	(±1.689)	(±0.17)	(±0.345)	(±1.049)	(±7.583)	(±103.021)	(±0.017)	(±0.328)	(±0.027)	(±0.208)	(±0.055)

[1]Indicates significant treatment main effects were observed.
[2]Indicates that significant interactions were shown to exist between location and treatment by the GLM.
[3]Indicates that significant main effect of location within the shell was observed.

at the shell edge, and higher ratios under ambient pCO_2 than elevated pCO_2 conditions (Fig. 2D; Table 1).

Post hoc comparisons also revealed that B:Ca, Mg:Ca, and Sr:Ca ratios differed significantly between the two locations analyzed in shells grown under ambient conditions, whereas significant differences in these *TE*:Ca ratios were not observed in shells grown under elevated pCO_2 (Figs. 2E–G, 3; Table 1). Exposure to high pCO_2 conditions effectively homogenized these *TE*:Ca ratios across the shell.

For Pb:Ca ratios, differences were only found between the two locations within the shell grown under elevated pCO_2 (Fig. 2H; Table 1). The pairwise comparisons revealed significant intra-shell differences in the U:Ca ratio in shell produced under both treatment and control conditions (Figs. 2I, 3A). The U:Ca ratios also differed significantly at the shell edge between the two CO_2 treatments, while no difference was found at the umbo.

The GLMs indicated that Al:Ca, Zn:Ca, Li:Ca, and Co:Ca ratios differed significantly between the two locations analyzed within shells (Figs. 2J–M, 3B; Table 1). Al:Ca and Zn:Ca ratios were found to be higher at the umbo than the edge under both CO_2 conditions (Fig. 2J,K; Table 1), whereas the Li:Ca ratio was higher at the shell edge than the umbo (Fig. 2l:Table 1. The Co:Ca ratio was, marginally yet significantly, higher at the edge than the umbo of shell produced under both CO_2 conditions (Fig. 2M).

The GLM showed a significant main effect of pCO_2 for Co:Ca, Ni:Ca, and Ti:Ca ratios (Figs. 2M–O, 3B). Both Co:Ca and Ni: Ca ratios were found to be lower in shell exposed to elevated pCO_2 conditions (Fig. 2M,N; Table 1), whereas Ti:Ca ratios were significantly higher in shells exposed to elevated pCO_2 conditions (Fig. 2O; Table 1).

Discussion

The results of this study showed that the incorporation of all, but three of elements analyzed were in some way affected by the CO_2 conditions to which animals were exposed. The effect of changes in CO_2 was most pronounced in shell formed when animals were older, with few elements affected in shell produced when animals were younger. These interactions between the CO_2 treatment to which animals were exposed and age at which shell material was deposited highlight the complex processes, which influence the incorporation of elements into bivalve shell. These results will likely have greater implications for the use of trace elements as climate proxies than for understanding larval dispersal patterns.

The interactive effects between the location analyzed in shells and the CO_2 treatment to which animals were exposed suggests that biological processes will affect how many elements are incorporated into shell under conditions of decreased pH. It has previously been found that under OA stress biological calcification processes will be affected (Cummings et al. 2011). The results of this study show that

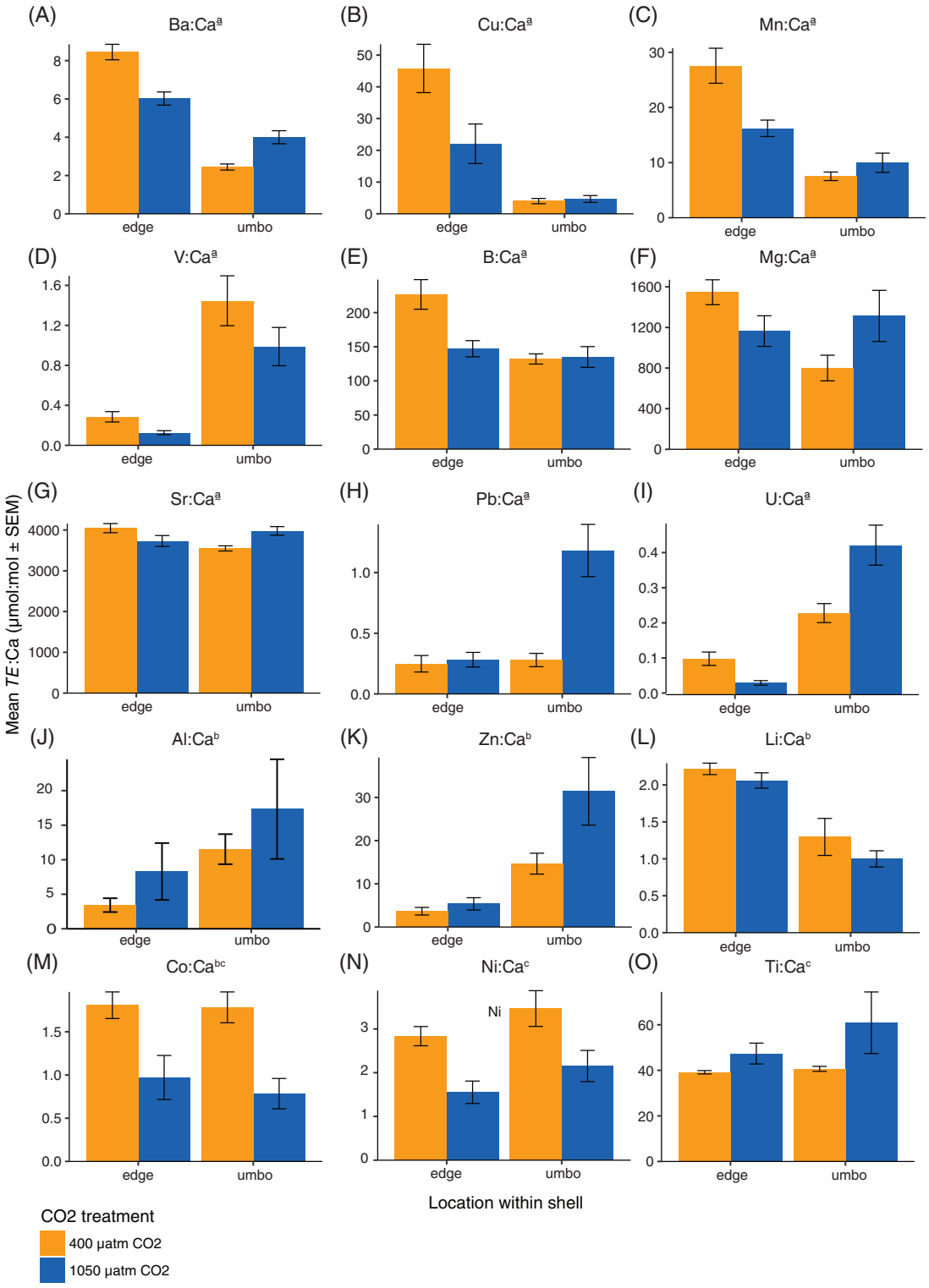

Fig. 2. Mean *TE*:Ca (±SEM) ratios at the two locations analyzed within *P. canaliculus* shell for each of the elements for which significant interaction or main effects were found. Note: superscript a indicates that GLMs showed significant interaction effects, b indicates a significant location main effect, and c indicates a significant pCO_2 treatment main effect as shown.

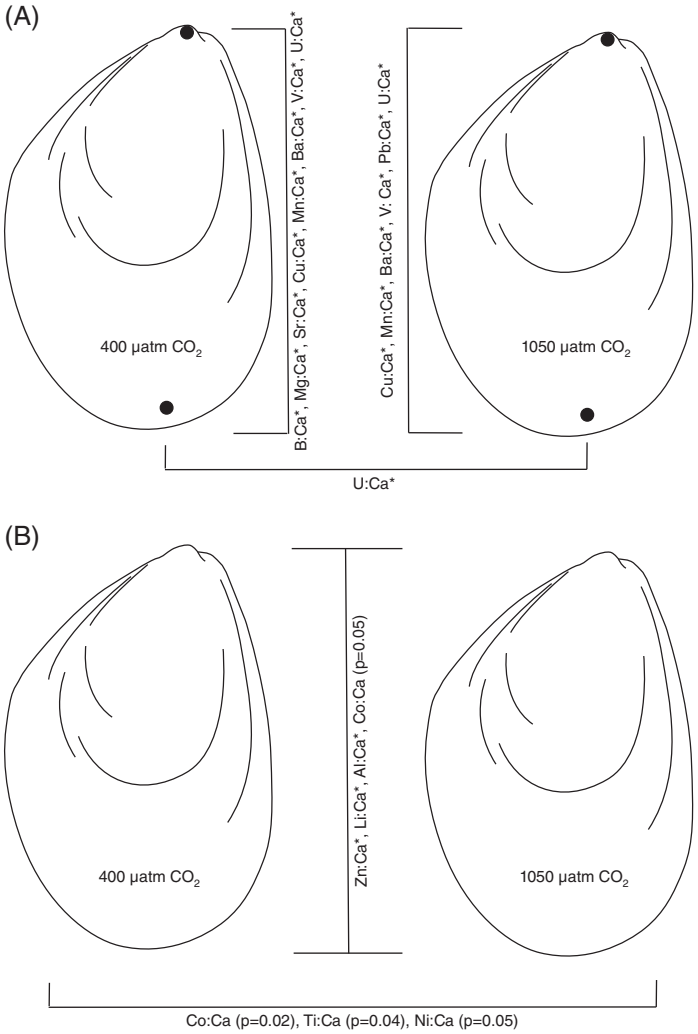

Fig. 3. *TE*:Ca ratios for which post hoc pairwise *t* tests with FDR correction showed significant differences ($\alpha = 0.05$) within shells or across pCO_2 treatments. (A) Pairwise differences shown by the post hoc t-test for elements where location:pCO_2 treatment interaction effects existed. (B) Pairwise differences for elements where no significant interaction term was found, but significant main effects of location or pCO_2 treatment were shown. Note:*$p < 0.01$

the age of the individual may mediate these effects. Although earlier life history stages are particularly sensitive to OA stress (Byrne and Przeslawski 2013), shell material at the umbo (produced when animals were younger) only differed in three *TE*:Ca ratios between treatments, whereas shell deposited later in life differed more substantially in its trace elemental composition. This raises the possibility of a survivorship bias where individuals, which are not able to calcify early shell with normal levels of trace elements do not survive. Latent effects of exposure to pH stress may, however, be present later in individuals life (Byrne and Przeslawski 2013). This along with the complex nature and direction of the interactions observed in this study indicate that the processes, which result in the incorporation of elements into bivalve $CaCO_3$ under OA conditions will be highly element specific.

The within shell differences observed for many elements in shells from both CO_2 treatments show that even in the absence of OA, stress elements are not incorporated consistently as animals age. It is possible that these changes in elemental incorporation are related to ontogenetic changes in the $CaCO_3$ polymorph produced (Weiss et al. 2002). It has also been suggested that growth rates may affect the incorporation of elements into bivalve shell (Strasser et al. 2008) which may explain why the *TE*:Ca ratios differed between shell produced early in life, when growth rates are faster, differed from that deposited later.

If using *TE*:Ca ratios in $CaCO_3$ structures to reconstruct environmental conditions it is important that the elements used have a direct relationship with pH and are not affected by biological factors. Although it has previously been suggested that U:Ca ratios in bivalve shell will serve as useful proxies of seawater pH (Frieder et al. 2014, Levin et al. 2015), this study showed biological changes may modify the relationship between pH and U:Ca ratios. In this study Co:Ca, Ni:Ca, and Ti:Ca ratios were shown to clearly and consistently differ across the shell between the two CO_2 treatments to which they were exposed. This suggests that these elements may serve as useful proxies for environmental pH. Nickel and cobalt show similarities which are likely to be responsible for pH changes being reflected in shell chemistry. In seawater, both of these elements are dominated by only two species, the free ion (Ni^{2+} and Co^{2+}), with the carbonate forms ($NiCO_3$ and $CoCO_3$) making up most of the remainder of these elements (Millero et al. 2009). Under the predicted future pH conditions used in this study, the portion of these elements in the carbonate forms is predicted to fall by approximately half (Milero et al. 2009). This fall is reflected in the results of this study, where the mean Ni:Ca and Co:Ca ratios in shells from treatment tanks were 58% and 48%, respectively, of those from control tanks. The behavior of Ti in response to pH changes is not well known due to low concentrations in seawater.

As only one environmental variable was manipulated in this study, it is important to establish that other conditions such as temperature or pollution do not play a greater role or interact with pH to influence the incorporation of these elements into bivalve shell. This is particularly the case as OA is unlikely to occur in isolation from other anthropogenic stressors (Byrne and Przeslawski 2013).

With regard to climate proxies, these results highlight that caution should be taken when selecting both elemental proxies and individuals for analysis. If comparing different individuals, care should be taken to ensure that they are analyzed in the same location within shells to ensure that ontogenetic differences in elemental incorporation are not misinterpreted as being due to changes in environmental conditions. Individuals

of a similar size should also be selected to reduce the possibility of biological changes influencing results.

Few elements were affected in the early shell material, which is used to reconstruct dispersal, by the CO_2 conditions to which they were exposed. This implies that reconstructing the dispersal trajectory and larval origin of individuals will remain largely unaffected by OA. The three elements that did differ in early stage shell of animals exposed to different CO_2 conditions (Co:Ca Ni:Ca, Ti:Ca, and U:Ca) have not previously been useful in assigning individuals to geographical locations or have provided only small increases in classification when included in a discriminant function analysis (Dunphy et al. 2011; Fodrie et al. 2011). When using trace elements to reconstruct dispersal trajectories, it is important that temporal stability in reference signals exists (Cathey et al. 2014). In the natural environment daily and seasonal swings in pH may occur (Law et al. 2017). These results show that these swings are unlikely to affect the early shell material and will not affect the temporal stability of these reference signals, although other seasonal changes may cause temporal instability.

Finally, the results of this study provide essential information that may allow the two primary applications in the field of trace elemental analysis of carbonate structures to be combined and open an exciting new avenue of research. The stability in the *TE*:Ca ratios at the umbo, which are generally used in trace elemental fingerprinting studies indicate that regardless of the pH in which the carbonate structure was deposited, its formation location will likely be able to be inferred. The *TE*:Ca ratios that are influenced by pH of seawater can then be examined to determine the carbonate chemistry of the water at which the carbonate structure was produced. It should be noted, however, that in the growing field of stable isotope analysis, the same ratios may be used reconstruct the properties of water masses (primarily nutrient dynamics) and estimate connectivity (Selleslagh et al. 2015). This suggests the response of stable isotope ratios to different environmental stressors and biology should be investigated in the future. In addition it has been shown that OA may have intergenerational (Parker et al. 2015), which will become a consideration over timescales longer than were investigated in this study. Nonetheless, provided the reference atlas of trace elemental fingerprints remains stable over time (Cathey et al. 2014), this may reduce the need for constant in situ sampling of seawater carbonate chemistry to determine how anthropogenic CO_2 emissions are affecting the world's oceans. Indeed, as multiple stressors are likely to interact to affect marine organisms (Byrne and Przeslawski 2013), it may be possible to reconstruct different environmental parameters using different *TE*:Ca ratios. This may allow individual exposure to varying environmental conditions at early life history stages to be inferred and the ecological consequences of this exposure to be better understood.

References

Becker, B. J., L. A. Levin, F. J. Fodrie, and P. A. McMillan. 2007. Complex larval connectivity patterns among marine invertebrate populations. Proc. Natl. Acad. Sci. U. S. A. **104**: 3267–3272. doi:10.1073/pnas.0611651104

Beer, N., S. Wing, and Y. Hu. 2011. Physical versus biological control of element incorporation into biogenic carbonate: an in situ experiment in a New Zealand fjord. Mar. Ecol. Prog. Ser. **433**: 289–301. doi:10.3354/meps09199

Byrne, M., and R. Przeslawski. 2013. Integrative and comparative biology multistressor impacts of warming and acidification of the ocean on marine invertebrates. Life Histories. **53**: 582–596. doi:10.1093/icb/ict049

Cathey, A. M., N. R. Miller, and D. G. Kimmel. 2014. Spatiotemporal stability of trace and minor elemental signatures in early larval shell of the northern Quahog (Hard Clam) Mercenaria mercenaria. J. Shellfish Res. **33**: 247–255. doi:10.2983/035.033.0124.

Cummings V, and others (2011) Ocean acidification at high latitudes: potential effects on functioning of the antarctic bivalve Laternula elliptica. PLoS One **6**, e16069. doi:10.1371/journal.pone.0016069

Dunphy, B. J., M.-A. Millet, and A. G. Jeffs. 2011. Elemental signatures in the shells of early juvenile green-lipped mussels (Perna canaliculus) and their potential use for larval tracking. Aquaculture **311**: 187–192. doi:10.1016/j.aquaculture.2010.12.016

Fodrie, F. J., B. J. Becker, L. A. Levin, K. Gruenthal, and P. A. McMillan. 2011. Connectivity clues from short-term variability in settlement and geochemical tags of mytilid mussels. J. Sea Res. **65**: 141–150.

Frieder, C. A., J. P. Gonzalez, and L. A. Levin. 2014. Uranium in larval shells as a barometer of molluscan ocean acidification exposure. Environ. Sci. Technol. **48**: 6401–6408. doi:10.1021/es500514j

Gattuso J-P, Hansson L (2011) *Ocean Acidification*, 1st ed., Oxford Univ. Press, Oxford, United Kingdom

Gomes, I., L. Peteiro, R. Albuquerque, R. Nolasco, J. Dubert, S. Swearer, and H. Queiroga. 2016. Wandering mussels: using natural tags to identify connectivity patterns among marine protected areas. Mar. Ecol. Prog. Ser. **552**: 159–176. doi:10.3354/meps11753

Hahn S, and others (2012) Marine bivalve shell geochemistry and ultrastructure from modern low pH environments: environmental effect versus experimental bias. Biogeosciences **9**:1897–1914. doi:10.5194/bg-9-1897-2012

Henehan MJ, and others (2013) Calibration of the boron isotope proxy in the planktonic foraminifera Globigerinoides ruber for use in palaeo-CO2 reconstruction. Earth Planet. Sci. Lett. **364**:111–122. doi:10.1016/j.epsl.2012.12.029

Hoffmann, L. J., E. Breitbarth, P. W. Boyd, and K. A. Hunter. 2012. Influence of ocean warming and acidification on

trace metal biogeochemistry. Mar. Ecol. Prog. Ser. **470**: 191–205. doi:10.3354/meps10082

Immenhauser, A., B. R. Schone, R. Hoffmann, and A. Niedermayr. 2016. Mollusc and brachiopod skeletal hard parts: intricate archives of their marine environment. Sedimentology **63**: 1–59. doi:10.1111/sed.12231

Jochum, K. P., U. Nohl, K. Herwig, E. Lammel, B. Stoll, and A. W. Hofmann. 2005. GeoReM : a new geochemical database for reference materials and isotopic standards. Geostand. Geoanalytical Res **29**: 333–338.

Kroll, I., A. Poray, B. Puckett, D. Eggleston, and F. Fodrie. 2016. Environmental effects on elemental signatures in eastern oyster Crassostrea virginica shells: using geochemical tagging to assess population connectivity. Mar. Ecol. Prog. Ser. **543**: 173–186. doi:10.3354/meps11549

Law CS, and others (2017) Ocean acidification in New Zealand waters: trends and impacts. New Zeal. J. Mar. Freshw. Res. **8330**:1–41. doi:10.1080/00288330.2017.1374983

Levin, L., B. Hönisch, and C. Frieder. 2015. Geochemical proxies for estimating faunal exposure to ocean acidification. Oceanography **25**: 62–73. doi:10.5670/oceanog.2015.32

Marr, J. P., J. A. Baker, L. Carter, A. S. R. Allan, G. B. Dunbar, and H. C. Bostock. 2011. Ecological and temperature controls on Mg/Ca ratios of Globigerina bulloides from the southwest Pacific Ocean. Paleoceanography **26**: 1–15. doi:10.1029/2010PA002059

Millero, F., R. Woosley, B. DiTrolio, and J. Waters. 2009. Effect of ocean acidification on the speciation of metals in seawater. Oceanography **22**: 72–85. doi:10.5670/oceanog.2009.98

Norrie, C., B. Dunphy, J. Baker, and C. Lundquist. 2016. Local-scale variation in trace elemental fingerprints of the estuarine bivalve Austrovenus stutchburyi within and between estuaries. Mar. Ecol. Prog. Ser. **559**: 89–102. doi:10.3354/meps11890

Parker, L. M., W. A. O'Connor, D. A. Raftos, H. O. Pörtner, and P. M. Ross. 2015. Persistence of positive carryover effects in the Oyster, *Saccostrea glomerata*, following transgenerational exposure to ocean acidification. PLoS One **10**(7): e0132276. https://doi.org/10.1371/journal.pone.0132276.

Poulain, C., D. P. Gillikin, J. Thebault, J. M. Munaron, M. Bohn, R. Robert, Y.-M. Paulet, and A. Lorrain. 2015. An evaluation of Mg/Ca, Sr/Ca, and Ba/Ca ratios as environmental proxies in aragonite bivalve shells. Chem. Geol. **396**: 42–50. doi:10.1016/j.chemgeo.2014.12.019

Ragg, N. L. C., N. King, E. Watts, and J. Morrish. 2010. Optimising the delivery of the key dietary diatom *Chaetoceros calcitrans* to intensively cultured Greenshell™ mussel larvae, *Perna canaliculus*. Aquaculture **306**: 270–280. doi:10.1016/j.aquaculture.2010.05.010

Selleslagh, J., H. Blanchet, G. Bachelet, and J. Lobry. 2015. Feeding habitats, connectivity and origin of organic matter supporting fish populations in an estuary with a reduced intertidal area assessed by stable isotope analysis. Estuar. Coasts **38**: 1431–1447. doi:10.1007/s12237-014-9911-5

Strasser, C. A., L. S. Mullineaux, and B. D. Walther. 2008. Growth rate and age effects on Mya arenaria shell chemistry: implications for biogeochemical studies. J. Exp. Mar. Biol. Ecol. **355**: 153–163. doi:10.1016/j.jembe.2007.12.022

Weiss, I. M., N. Tuross, L. Addadi, and S. Weiner. 2002. Mollusc larval shell formation: amorphous calcium carbonate is a precursor phase for aragonite. J. Exp. Zool. **293**: 478–491. doi:10.1002/jez.90004

Yu, J., H. Elderfield, and B. Honisch. 2007. B/Ca in planktonic foraminifera as a proxy for surface seawater pH. Paleoceanography **22**. doi:10.1029/2006PA001347

Acknowledgments

The authors would like to thank Stuart Morrow of The University of Auckland ICP-MS center for assistance with laser analyses. CN was supported by a UoA Doctoral Scholarship. Kevin Chang from the UoA statistical consulting center provided invaluable statistical advice. Joel Baker also provided useful advice. Biological trials were conducted under the Coastal Acidification, Rate, Impacts and Management (CARIM) program, funded by the NZ Ministry of Business, Innovation and Employment (C01X1510) using mussels bred and characterized as part of the Cawthron Cultured Shellfish program (CAWX1315). NIWA Coasts and Oceans Program (COME1902) provided funding LA-ICP-MS Analyses. The authors would like to thank the CARIM and SpatNZ teams for their enthusiastic support throughout this project. We would also like to thank the editors and two reviewers whose feedback greatly improved this manuscript.

Submitted 15 January 2018
Revised 10 April 2018
Accepted 22 June 2018